

UNITED STATES DEPARTMENT OF THE INTERIOR
GEOLOGICAL SURVEY

Reconnaissance Geophysics in the Clifton and Gillard
Geothermal Areas, SE Arizona

by

D. Klein, C. Long, K. Christopherson, and F. Boler

U.S.G.S. Open File Report 80-325

1980

Reconnaissance Geophysics in the Clifton and Gillard
Geothermal Areas, SE Arizona

Table of Contents

	Page
Introduction	1
AMT Data	3
Gillard Data	4
Clifton Data	8
Telluric Data	9
Gravity and Aeromagnetics	9
Discussion	14
References	16
Appendix 1: AMT Data Log, Gillard	18
Appendix 2: AMT Data Log, Clifton	19

List of Figures

Fig. 1. AMT/Telluric Station Localities	2
Fig. 2. AMT Apparent Resistivities, Gillard 1 and 2	5
Fig. 3. AMT Apparent Resistivities, Gillard 3	6
Fig. 4. AMT Apparent Resistivities, Clifton 1 and 2	7
Fig. 5. Clifton Telluric Line	10
Fig. 6. Complete Bouguer Gravity Residual Map	11
Fig. 7. Residual Aeromagnetic Intensity Map	13

Reconnaissance Geophysics in the Clifton and Gillard

Geothermal Areas, SE Arizona

U.S.G.S. Open File Report 80-325

D. Klein, C. Long, K. Christopherson, and F. Boler

Introduction

Five audio-magnetotelluric (AMT) stations (7.5 to 18,600 Hz) and a single telluric line (0.033 Hz) were established in the vicinity of Clifton and Gillard hot springs, Arizona (fig. 1). The area of these measurements is centered at about 33° north latitude and 109°18' west longitude. These data were obtained as part of the U.S. Geological Survey (USGS) program to make reconnaissance evaluations of potential economic geothermal resources in Known Geothermal Resource Areas (KGRAs).

The Clifton hot springs, about one mile north of Clifton on the San Francisco River, are reported to have temperatures ranging from 59°C at the surface to an estimated 140°C below the surface; the Gillard hot springs, located about one mile east of the Gila-San Francisco River junction, are reported to have surface temperatures 82°C and about 140°C below the surface. (White and Williams, 1975, p. 26-27; Muffler, 1979, p. 62-63.)

The present measurements detect subsurface resistivities in the survey areas that are in the range (~4-7 ohm-m) to suggest the inference that geothermal conditions exist within the zone of electromagnetic probing (the skin depths at 7.5 Hz range from 0.4 to 2.0 km for these resistivities). The resistivities, especially in the Gillard area (~7 ohm-m) are ambiguous with regard to geothermal potential because the main mass of rock is consolidated alluvium which often has intrinsic low

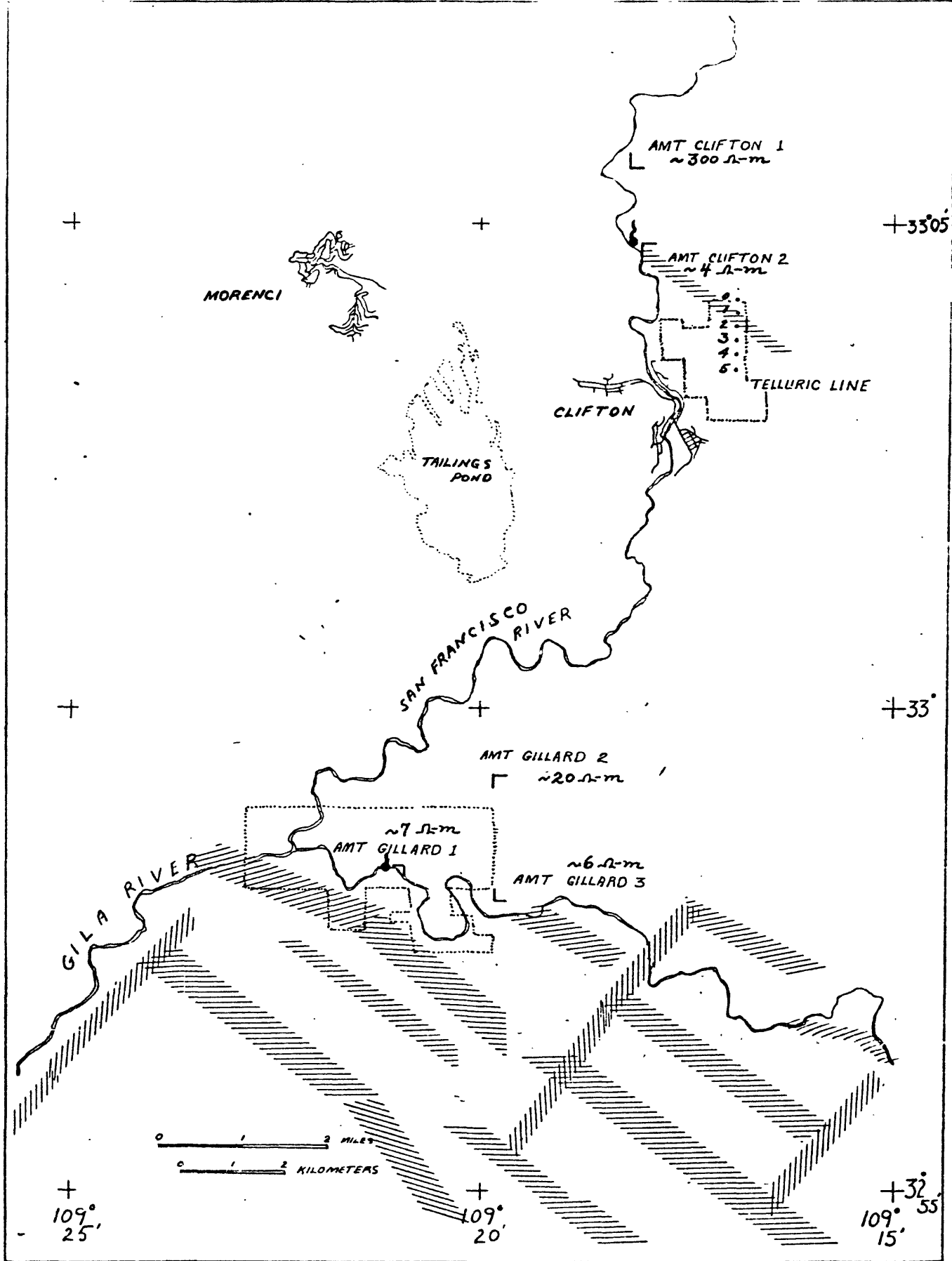


Figure 1.--AMT/telluric station localities and 7.5 Hz apparent resistivities ($\Omega\text{-m}$), Known Geothermal Resources Areas (dotted), hot springs, (δ) and probable fault zones (hachured).

resistivity. It would seem that a large volume of hot water (over 150°C) within the zone of penetration would have caused lower resistivities than observed; thus the data do not warrant emphasis on the idea that a highly productive reservoir at shallow depth exists within either area. However, the data are inadequate to dismiss the possibility of deep hot reservoirs, or the possibility that significant amounts of moderately warm geothermal waters may be tapped at economical depth. Geochemical investigations by the Geothermal Group of the Arizona Bureau of Geology and Mineral Technology indicate that the latter is a significant possibility for both areas (Witcher, 1979a, 1979b). Structural conditions, inferred from the present data in conjunction with previous USGS aeromagnetic and gravity data, indicate that the source of the thermal waters are relatively narrow conduits, formed by basin faulting, most likely striking northwest and probably circulating hot water derived from great depth.

AMT Data

AMT data was measured at frequencies from 7.5 to 18,600 Hz using equipment and procedures described by Hoover, Frischknecht, and Tippens (1976), Hoover and Long (1976), and Hoover, Long, and Senterfit (1978). Two orthogonal sets of magnetic (H) and electric (E) field amplitudes were recorded on chart paper for each of the band passed frequencies. Simultaneous peaks from each set were scaled and reduced to scalar apparent resistivity (ohm-m) for north-south E (ρ_{xy}) and east-west E (ρ_{yx}). The geometric mean of these data, the number of samples used for each estimate, and the 95 percent confidence level are tabulated in appendices 1 and 2. The confidence level is listed as a percentage of a log cycle.

The data are plotted versus frequency in Figures 2-4. Vertical bars represent the 95 percent confidence limits; for points with question marks there were too few samples to reliably estimate this parameter.

Confidence levels in these data measure statistical consistency in the estimates, but they do not necessarily provide accurate uncertainties in apparent resistivity. At a particular frequency there may be consistent bias in the measured fields that relates to cultural electromagnetic signals or peculiarities in the natural signal (for instance, deviations from the assumption of a uniform H-field that is used to derive the apparent resistivity equation); the 10 and 14 Hz data at the Gillard Hot Springs stations 2 and 3 are examples of this. Such large apparent resistivity excursions are not expected over a frequency interval of 4 Hz even for conditions of intense geologic complexity. Thus, for interpretation, such data are rejected as unrealistic estimates of earth response to plane wave fields.

Gillard Data

In general, these data show low apparent resistivities at the more deeply penetrating frequencies (below 76 Hz; 3-12 ohm-m at stations 1 and 3; 8-50 ohm-m at station 2). Station 1 was located over the hot springs, on a sandy river bottom area. The consistent low resistivity over the entire frequency range reflects probably warm, fluid saturated alluvium throughout the depth of penetration. Station 3 was located on consolidated alluvium on a 200 foot bank above the river bottom. The large scatter reflects topographic effects and possible subsurface inhomogeneity, but the average of the data at the lower frequency indicates a situation similar to that at station 1. Station 2 was located

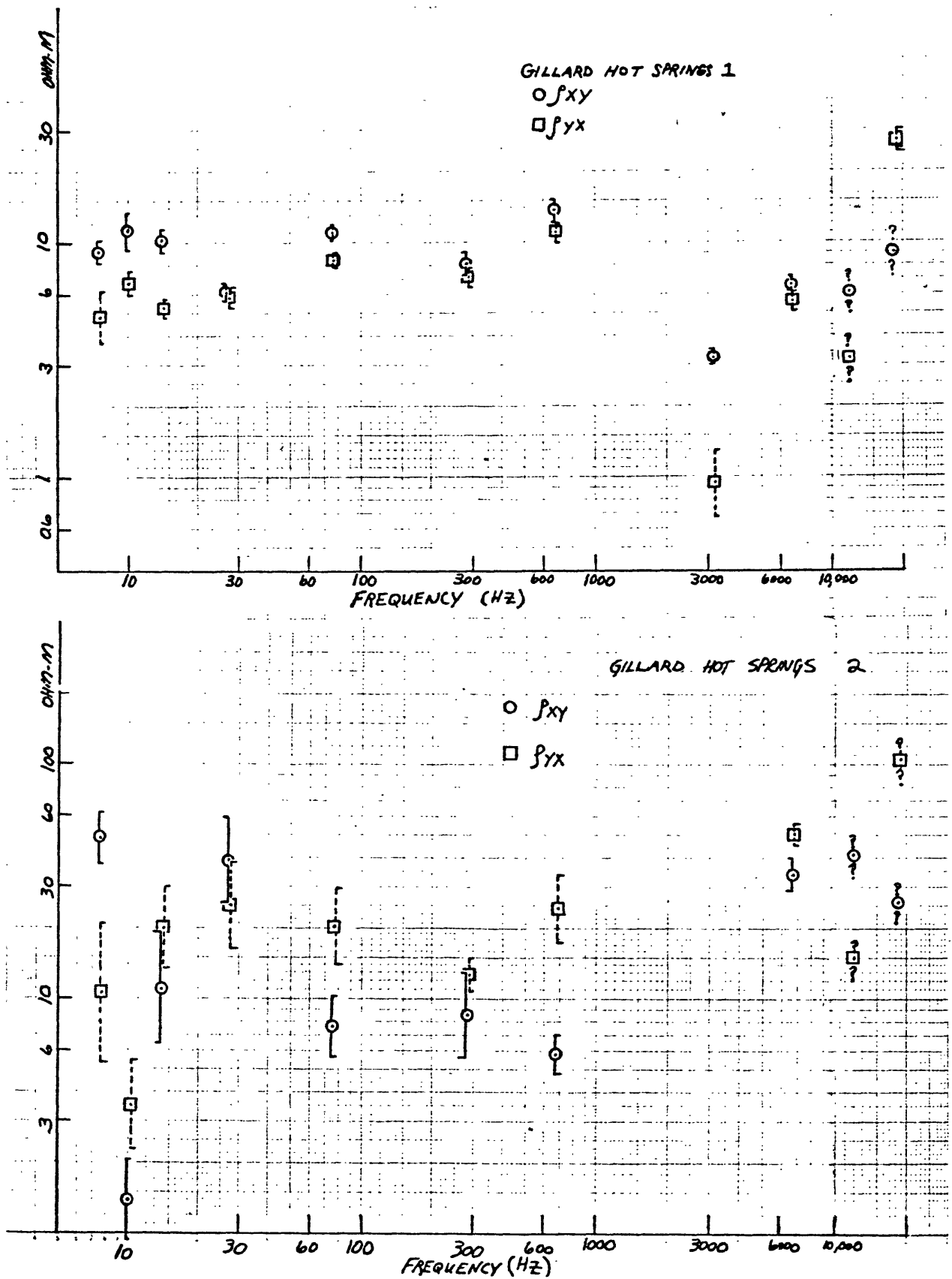


Figure 2.--Gillard stations 1 and 2 AMT apparent resistivity data versus frequency data with 95 percent confidence bars; dashed for ρ_{yx} ; question marks where confidence limits not established. ρ_{xy} , E_x/H_y ; ρ_{yx} , E_y/H_x data.

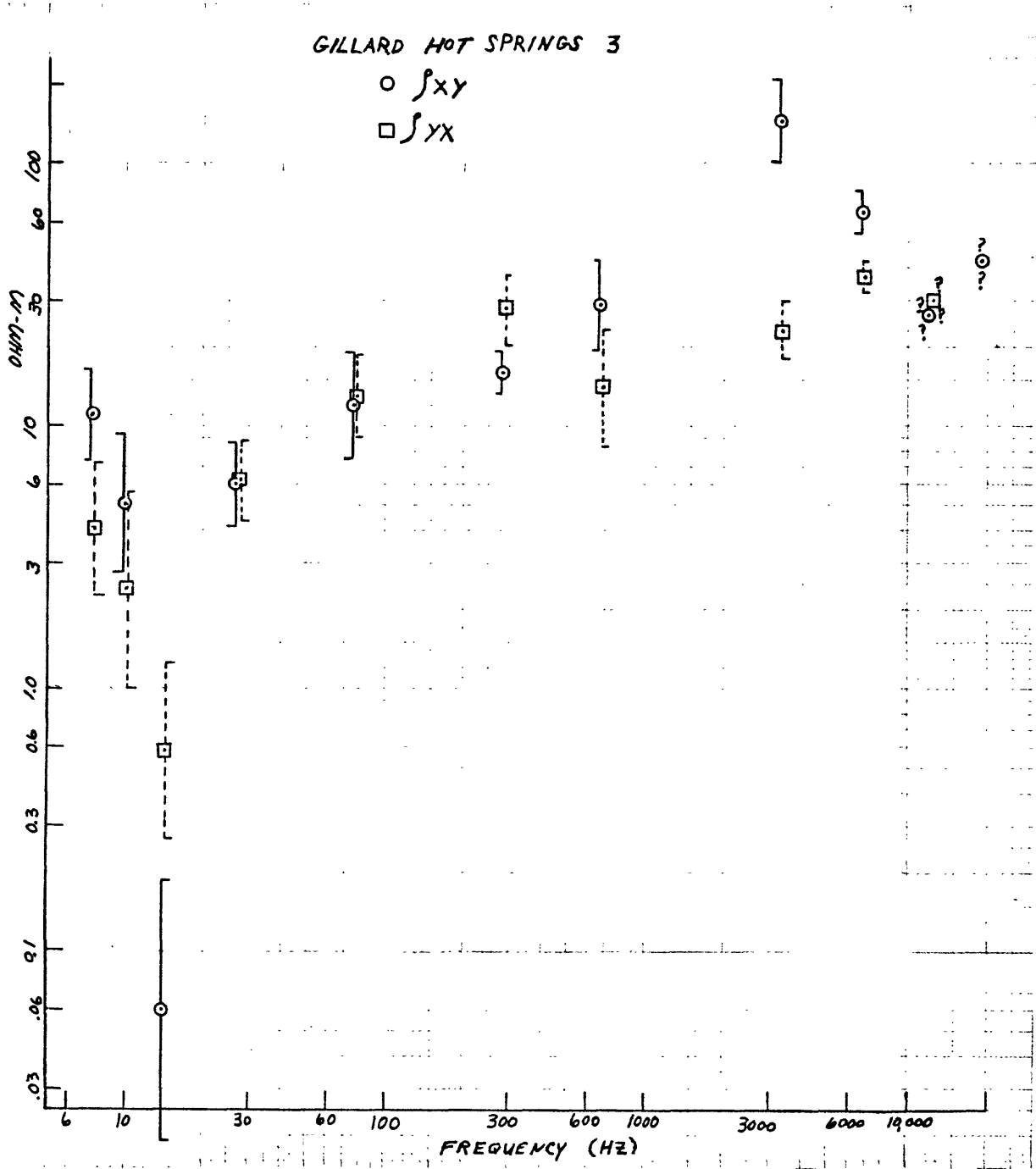


Figure 3.--Gillard station 3 AMT apparent resistivity data versus frequency data with 95 percent confidence bars; dashed for ρ_{yx} ; question marks where confidence limits not established. ρ_{xy} , E_x/H_y ; ρ_{yx} , E_y/H_x data.

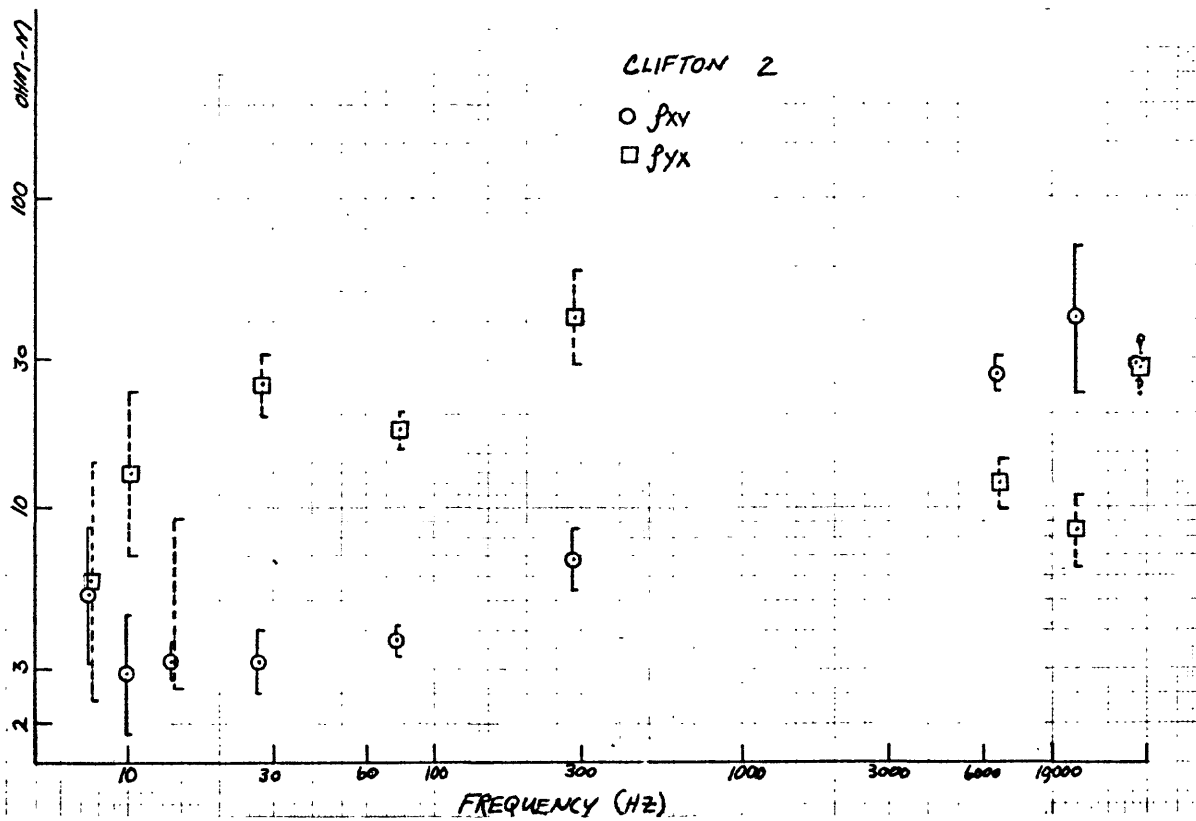
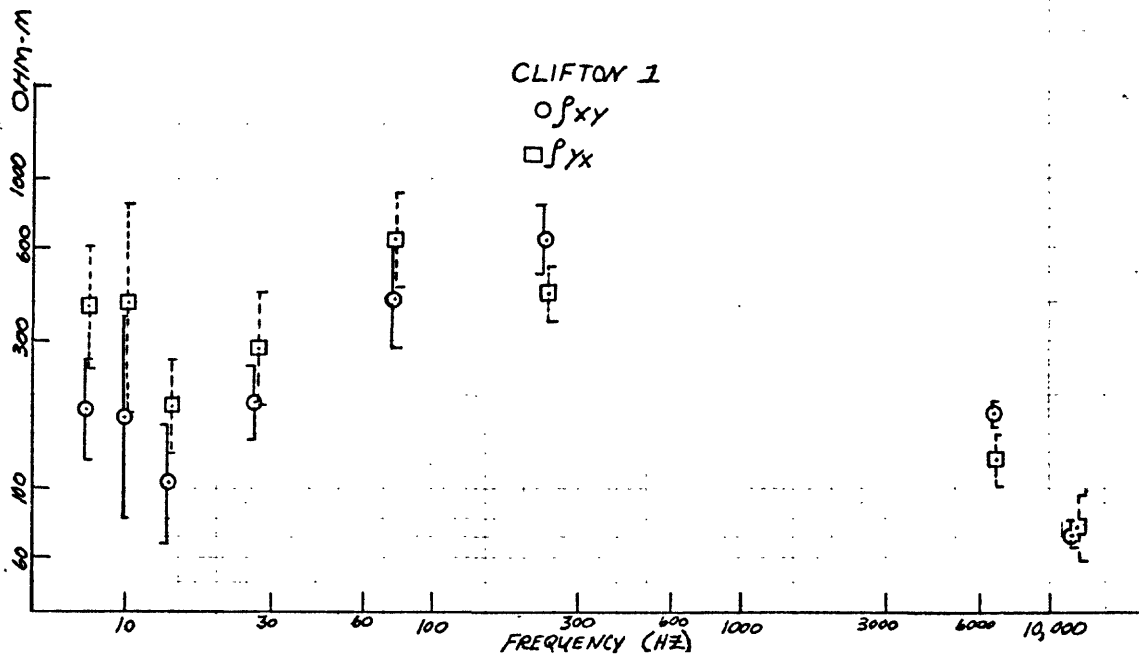


Figure 4.--Clifton stations 1 and 2 AMT apparent resistivity data versus frequency data with 95 percent confidence bars; dashed for ρ_{yx} ; question marks where confidence limits not established. ρ_{xy} , E_x/H_y ; ρ_{yx} , E_y/H_x data.

on a 300 foot hill, on consolidated alluvium, about 1 1/2 mi north of the river bottom. The data above 1000 Hz is distorted by surface topography but smooths out to reflect resistivities of about 10 ohm-m or less in the more deeply sensed subsurface material.

Clifton Data

Station 1 is located about 1 mile north of the hot springs in an area of crystalline rock. The data shows generally high resistivity throughout the frequency range which suggests the absence of geothermal fluid saturated rock. The possible resistivity decrease from about 500 ohm-m at 70-270 Hz to about 150 ohm-m at 7.5 to 14 Hz is probably reflecting normal ground-water conditions; however, such a drop in the resistivity of crystalline rock at depth is not the norm and the possibility that the data is sensing a zone of hydrothermal alteration cannot be rejected. Station 2 is located on the hot springs area, and is close to the contact between basin alluvium and crystalline rock. The E-field line for ρ_{yx} went up a 400 foot incline while that for ρ_{xy} was parallel to and on the river bed. Because of topographic and structural effects, ρ_{xy} is interpreted to give a more accurate measure of the average resistivity variations than ρ_{yx} . The apparent resistivity, ρ_{xy} , goes to about 3 ohm-m in the lower frequencies. This is consistent with a warm water saturated zone below the springs. Witcher (1979a, b) notes that the water discharges in the Clifton area have higher than normal salinity; this condition could account for the observed resistivities without hypothesizing abnormal thermal effects.

Telluric Data

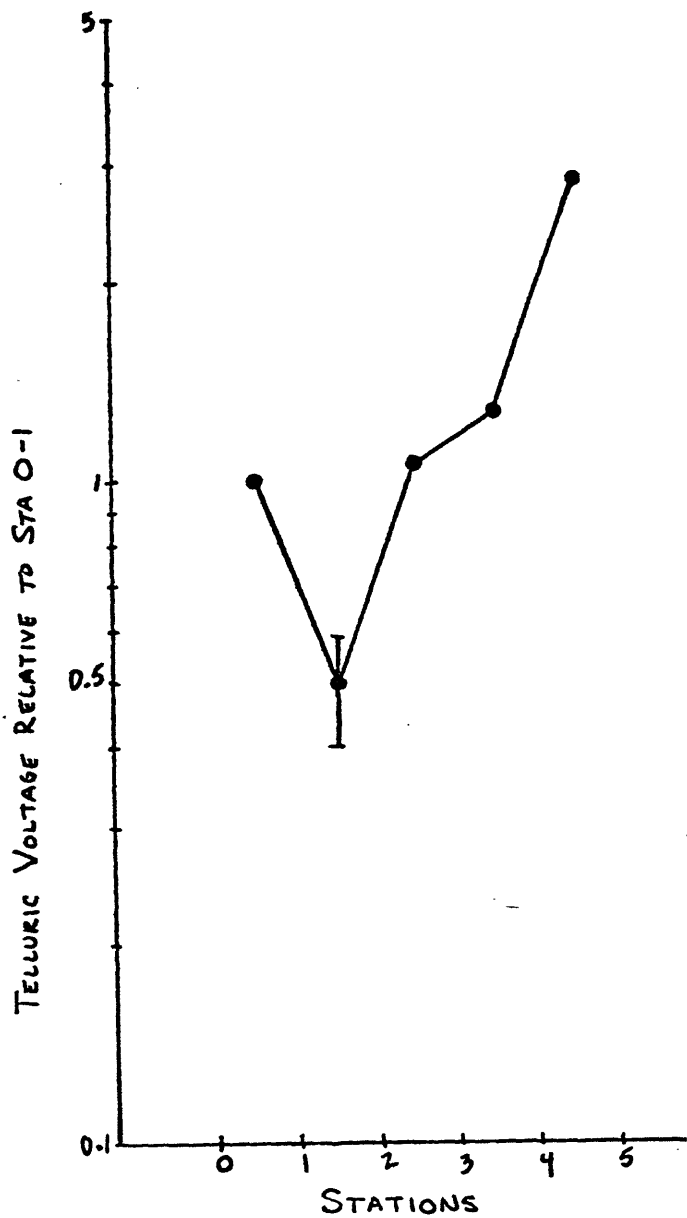
A telluric line (E-field ratio method) was established within the northeast part of the K.G.R.A. just east of Clifton (fig. 5). Severe topography and high water in the Gila River precluded a similar line in the Gillard area. The equipment and measurement procedure was similar to that described by Beyer (1977). Measurements were made at a frequency bandwidth of 0.020 to 0.045 Hz using in-tandem, north-south, electrode pairs with electrode separations of 500 m.

Figure 5 shows the relative voltage ratios based on the first dipole. These data are identically equivalent to the square root of apparent resistivity changes along the profile assuming that the electromagnetic fields are not distorted by lateral changes in resistivity along the profile.

The value of the electric field ratio between points 1 and 2 is presumably indicative of a fairly narrow and pronounced resistivity low. The standard deviation of the data for this measurement shows that measurement statistics cannot account for the variation.

Gravity and Aeromagnetics

Figure 6 is a complete bouguer gravity map of the area (Boler and others, 1980). The contour interval of 2 mgal is on the fringe of the estimated error, but the overall trends are considered reliable. The main features reflect the general geologic units in the area, (Wilson and others 1969). Northwest of the Gila and San Francisco Rivers, the geology is dominated by a major Laramide intrusive reflected by a broad gravity high. The shape of this broad gravity high is poorly defined due to the sparsity of stations northwest of the San Francisco River; in particular,



TELLURIC PROFILE
CLIFTON AZ KGRA

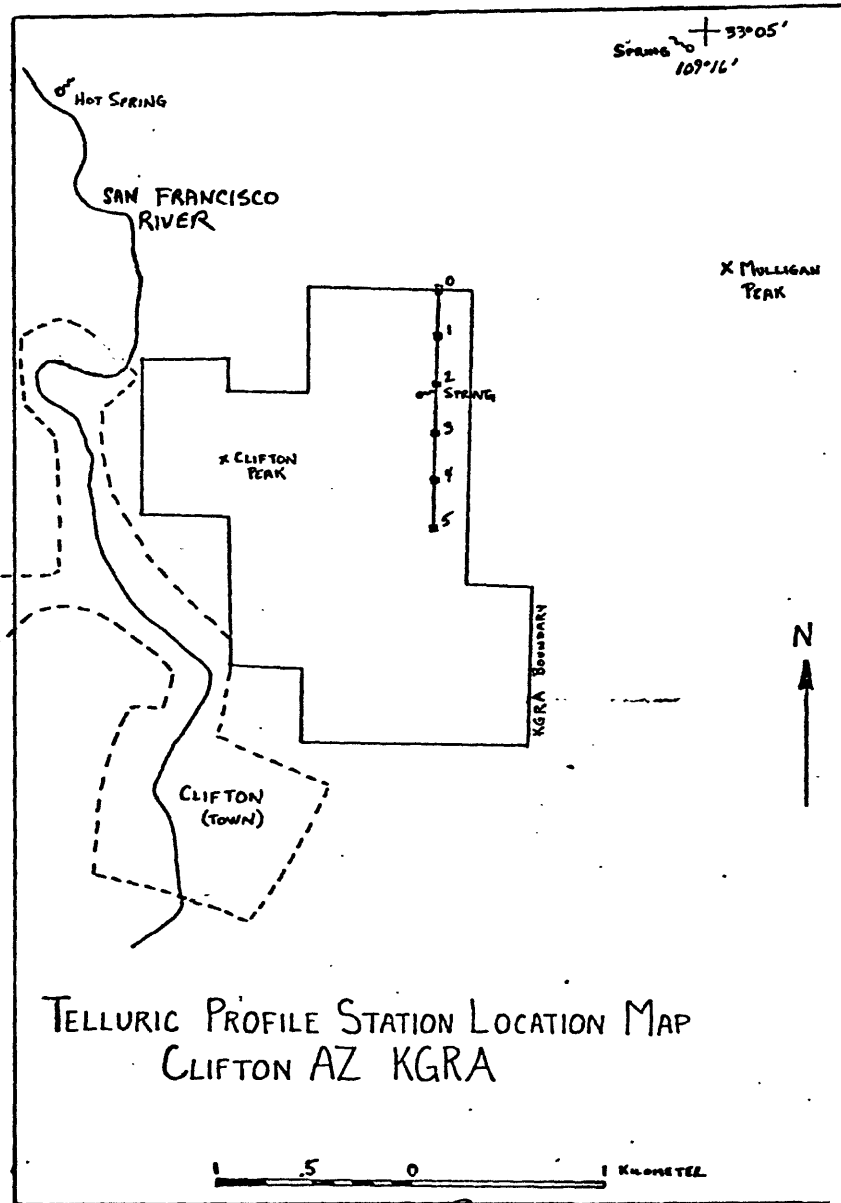
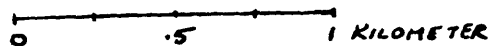


Figure 5.--Telluric line voltage ratios and station locations in the Clifton area.

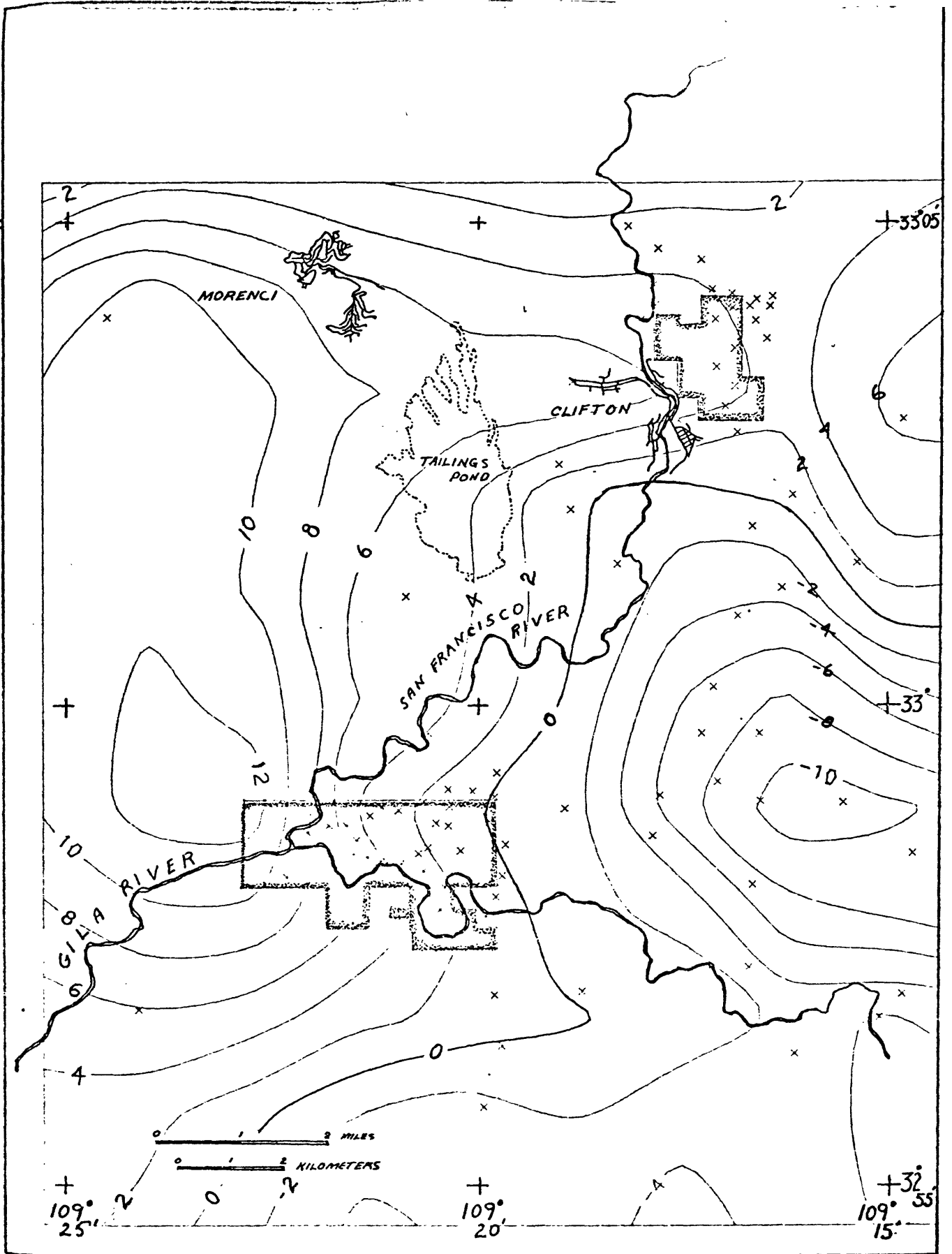


Figure 6.--Complete Bouguer gravity residual map. Contour interval, 2 mgal; x, station locations (Boler and others 1980).

one can not place much confidence on the apparent pattern of the gravity maximum based on the present distribution of stations. South of the Gila River the area is covered by Tertiary and Quaternary volcanics, with the gravity being rather expressionless. North of the Gila, extending roughly to the zero anomaly contour, the surface material is Quaternary basin fill reflected by a major gravity low. The main boundaries of the basin block inferred from a qualitative examination of gravity and aeromagnetics, roughly coincides on the southwest with the Gila River and on the northeast with the zero bouguer contour. Northeast of this block crystalline igneous rocks are exposed.

Figure 7 is a composite of two residual intensity aeromagnetic maps (U.S. Geological Survey, 1970, 1972, 1979). The apparent discontinuity at 33°N. latitude was created because of different survey specifications: on the top, 1 mile flight line spacing at a barometric altitude of 10,500 feet was used (U.S. Geological Survey, 1970) and on the bottom, 1/2 mile spacing at 1500 feet above mean ground elevation was used (U.S. Geological Survey, 1979). The effect of the Laramide intrusive dominates the magnetic intensity pattern to the northwest; nearly featureless long wavelength patterns dominate the basin north of the Gila River, and complex northeast and northwest trends dominate the field south of the Gila-San Francisco Rivers. The latter patterns form the basis for the structural features (fig. 1) being interpreted as a series of parallel faults successively displaced down to the northeast. A pronounced magnetic low generally just south of the Gila River may in part be influenced by hydrothermal alteration and have geothermal significance beyond that of a fault-induced magnetic contact. The northwest structural

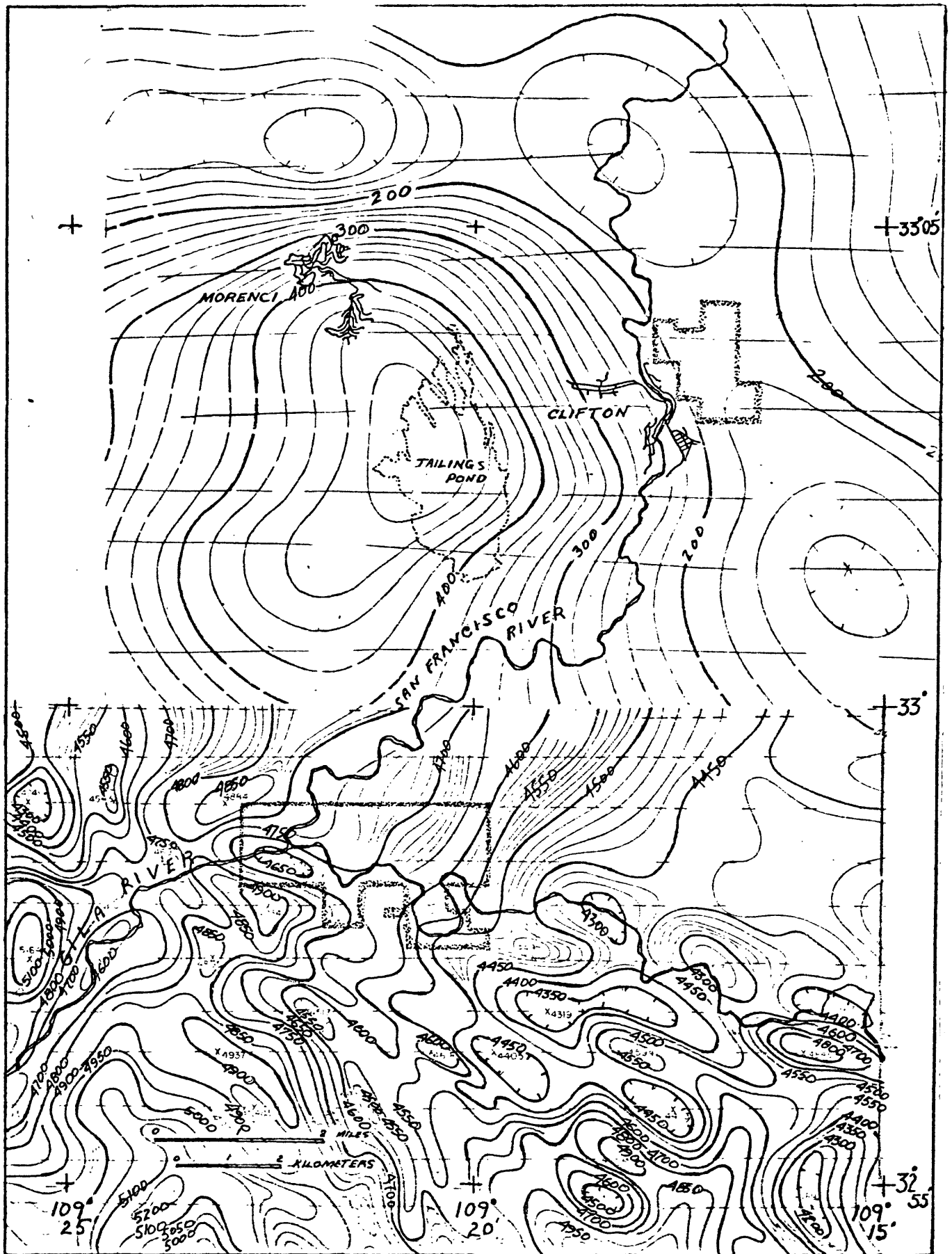


Figure 7.--Residual aeromagnetic intensity map. Data from U.S. Geological Survey (1970, 1972, north of 33°N, 10,500' altitude; 1979, south of 33°N, 1,500' altitude). Flight lines shown by broken lines.

patterns south of the Gila River terminate at the junction of the Gila and San Francisco Rivers and along the Gila River to the Southwest. This may provide evidence for an intersecting crustal weakness that influences the concentration of thermal fluid migration in the area of Gillard hot springs.

Discussion

Apparent resistivities from 7.5 Hz AMT data are marked by their respective station in figure 1. These are representative of the deeper resistivities sensed by the measurements. The values listed are mid-region between the ρ_{xy} and ρ_{yx} data with an uncertainty of about 1/2 log cycle. The low values at Clifton Station 2 and Gillard Stations 1 and 3 are noteworthy.

Also shown on Figure 1 are fault zones inferred from the aeromagnetic data. With the exception of the zone crossing the telluric line, these were chosen along quasi-linear gradients in the magnetic intensity; the high is to the southwest and (or) southeast and the low is to the northeast or northwest.

The zone crossing the telluric line is mainly dependent on the results of the voltage ratio anomaly. Its directional trend, however, is chosen to coincide roughly with the northwest boundary of the basin as defined by gravity data and with the Clifton hot springs location.

Based on the structure inferred from magnetics, the Gillard area is straddling the north edge of a sequence of basin-forming faults. It is probable that these extend deep enough to form the source passages for the hot spring fluids. It is not known whether stratigraphic conditions could favor the formation of a geothermal reservoir in this area but the AMT

data does not strongly indicate a voluminous, high-temperature zone within the range of probing. Resistivities of 6-7 ohm-m may be thermally induced in this area, but similar AMT apparent resistivities have been commonly observed by C. Long in other basin environments in the southwest United States where no thermal manifestation exists. Wynn and Zonge (1975) also report low apparent resistivities from controlled source experiments in Arizona basin sediment sections, for instance 0.3-3 ohm-m at Wilcox Playa and 5-30 ohm-m in Quaternary and Tertiary alluvium and Tertiary volcanics near Safford. The possibility of thermal origin for the resistivities at Gillard stations 1 and 3 should not be discarded because Station 2 shows somewhat higher resistivity in similar rock type of the same area. The thermal manifestations are interpreted as being the result of a rather narrow northwest trending fluid conduit extending to depth great enough to tap hot water. There is need for further investigations in the area, particularly because of the likelihood of the existence of medium temperature water (100-150°C) water in moderate quantities along the inferred faults near the Gila River.

A similar situation is believed to exist in the Clifton thermal system. An interpretation of the structural pattern here could be improved with more detailed gravity and magnetic data. Electrical surveys could also be highly informative but would be expensive because of the difficult access to suitable observation points.

References

- Boler, F. M., Klein, D, Christopherson, K., and Hoover, D., 1980, Gravity observations-Clifton-Morenci area, Greenlee County, SE Arizona: U.S.Geological Survey Open-File Report no. 80-96, 18 p.
- Beyer, J. H., 1977, Telluric and D.C. resistivity techniques applied to the geophysical investigation of Basin and Range Geothermal Systems, Part I, the E-field Ratio Telluric Method: Lawrence Berkeley Laboratory, U. California Report LBL-6325 (3 parts).
- Hoover, D. B., Frischknecht, F. C., and Tippens, C. L., 1976, Audio-magnetotelluric sounding as a reconnaissance exploration technique in Long Valley, California: Journal of Geophysical Research, v. 81, 801-809.
- Hoover, D. B., and Long, C. L., 1976, Audio-magnetotelluric methods in reconnaissance geothermal exploration, in Proceedings 2nd United Nations Symposium Development Geothermal Resources: p. 1059-1064.
- Hoover, D. B., Long, C. L., and Senterfit, R. M., 1978, Some results from audio-magnetotelluric investigations in geothermal areas: Geophysics, v. 43, no. 7, p. 1501-1514.
- Muffler, L.J.P., ed., 1979, Assessment of Geothermal Resources of the United States-1978: U.S. Geological Survey Circular 790, 163 p.
- U. S. Geological Survey, 1970, Aeromagnetic map of the Morenci-Monticello area, southeastern Arizona and southwestern New Mexico, Sheet 2 of USGS Open file G71334 (1:62,500).
- U. S. Geological Survey, 1972, Aeromagnetic map of the Morenci-Monticello area, Southeastern Arizona. U.S. Geological Survey Geophysical Investigations Map GP-838, scale 1:250,000.

- U.S. Geological Survey, 1979, Aeromagnetic map of the north and west parts of the Silver City 1° by 2° quadrangle, New Mexico and Arizona; Open-File Report 79-1452, scale, 1:62,500.
- White, D. E., and Williams, D. L., eds, 1975, Assessment of geothermal resources of the United States--1975: U.S. Geological Survey Circular 726, 155 p.
- Wilson, E. D., Moore, R. T., and Cooper, J. R., 1969, Geologic Map of Arizona; U.S. Geological Survey and Arizona Bureau of Mines, scale, 1:500,000.
- Witcher, J. C., 1979a, A progress report of geothermal investigations in the Clifton area in Hahman, W. R., Sr., Geothermal Reservoir Site Evaluation in Arizona; Bureau Geology Mineral Technology, Tucson, Arizona, Semiannual Progress Report for the Period July 15, 1978 - Jan. 15, 1979, Tucson, Arizona, p. 26-41.
- _____ 1979b, A geothermal reconnaissance study of the San Francisco River between Clifton, Arizona and Pleasanton, New Mexico in Hahman, W. R., Sr., Geothermal Reservoir Site Evaluation in Arizona; Bureau Geology Mineral Technology, Tucson, Arizona, Progress Report for the period January 16 to November 1, 1979, p. 156-173.
- Wynn, J. C., and Zonge, K. L., 1975, EM coupling, its intrinsic value, its removal and the cultural coupling problem: Geophysics, v. 40, p. 831-850.

pa = observed apparent resistivity in ohm-meters

N = number of observations

Er = 95% confidence limit: ~ % log cycle - = no data

"NOTE" - Telluric line orientation indicated with station numbers.

Sta. No.		FREQUENCY											
		7.5	10	14	27	76	285	685	1.2K	3.3K	6.7K	10.2K	18.6K
Ex/Hy 1	pa	9.1	11.1	10.1	6.1	11.0	8.1	13.6	-	3.4	6.6	-	9.0
	N	9	12	7	9	11	11	7	-	6	7	-	7
	Er	5%	8%	5%	3%	3%	5%	5%	-	3%	2.4%	-	1%
Ey/Hx	pa	4.8	6.8	5.3	5.8	8.3	7.1	3.0	-	.93	5.6	-	(27)
	N	11	8	10	9	11	9	11	-	6	7	-	7
	Er	11%	5%	4%	4%	3%	6%	4%	-	14%	4.1%	-	3%
Ex/Hy 2	pa	4.8	1.4	11	39	7.6	8.6	5.9	-	-	34	(41)	(26)
	N	5	7	7	9	13	13	10	-	-	10	3	5
	Er	10.5%	17.1%	24.1%	18.8%	13.2%	18%	8.9%	-	-	7%	25%	1%
Ey/Hx	pa	10.4	3.5	15	25	20.2	12.8	24.7	-	-	51	(15)	(105)
	N	7	5	7	9	20	9	10	-	-	7	3	5
	Er	29%	19.1%	17.1%	18.4%	16.6%	7.1%	14.5%	-	-	3.8%	53%	2%
Ex/Hy 3	pa	11.0	5.00	.06	6.0	12	16	29	-	142	65	(26)	(42)
	N	7	9	5	9	10	6	6	-	6	7	4	3
	Er	16.5%	26.7%	49%	16%	20%	8%	17%	-	16%	8%	4%	1%
Ey/Hx	pa	4.2	2.4	.58	6.2	13	28	14	-	23	37	30	?
	N	8	8	5	9	10	6	9	-	6	7	4	-
	Er	25.3%	37.3%	33%	15%	16%	13%	22%	-	11%	6%	4%	-
	pa												
	N												
	Er												
	pa												
	N												
	Er												

ρ_a = observed apparent resistivity in ohm-meters

N = number of observations

Er = 95% confidence limit; % log cycle - = no data

"NOTE" - Telluric line orientation indicated with station numbers.

Sta. No.		FREQUENCY											
		7.5	10	14	27	76	285	685	1.2K	3.3K	6.7K	10.2K	18.6K
Ex/Hy 1	ρ_a	180	170	105	190	405	640	—	—	—	174	71	—
	N	13	9	12	12	10	15	—	—	—	8	7	—
	Er	16%	32%	19%	12%	16%	11%	—	—	—	4%	4%	—
Ey/Hx	ρ_a	391	399	186	283	648	422	—	—	—	123	74	—
	N	13	9	12	12	11	15	—	—	—	8	7	—
	Er	20%	33%	15%	18%	15%	9%	—	—	—	8%	11%	—
Ex/Hy 2	ρ_a	5.2	2.9	3.2	3.2	3.7	6.8	—	—	—	27	41	29
	N	8	10	8	9	10	14	—	—	—	10	6	4
	Er	22%	19%	6%	10%	5%	10%	—	—	—	6%	23%	1%
Ey/Hx	ρ_a	5.8	13	4.9	25	18	51	—	—	—	12	8.4	28
	N	8	11	8	9	10	14	—	—	—	10	6	4
	Er	38%	26%	27%	10%	6%	15%	—	—	—	8%	12%	2%
	ρ_a												
	N												
	Er												
	ρ_a												
	N												
	Er												
	ρ_a												
	N												
	Er												